The Fate of the Formic Acid Proton on the Anatase TiO2(101) Surface

Erika Fallacara, Fabio Finocchi, Marco Cazzaniga, Stéphane Chenot, Slavica Stankic, Michele Ceotto

How to cite: Angew. Chem. Int. Ed. 2024, e202409523
doi.org/10.1002/anie.202409523

Surface Chemistry

The Fate of the Formic Acid Proton on the Anatase TiO_2(101) Surface

Erika Fallacara, Fabio Finocchi, Marco Cazzaniga, Stéphane Chenot, Slavica Stankic, and Michele Ceotto**

Abstract: As a prototype adsorption reaction of gas Brønsted acid on oxides, we study the adsorption of formic acid on anatase. We perform infrared spectroscopy measurements of adsorbed HCOOH and HCOOD on TiO_2 nanopowders, from 13 K up to room temperature in an ultra-high vacuum chamber. We assign the IR signals via computed spectra from nuclear quantum dynamics simulations using our divide-and-conquer semiclassical ab initio molecular dynamics method. The acid proton forms an extraordinarily short and strong hydrogen bond with the surface oxygen. The strength of this hydrogen bond, that compares to H bonds in ice at high pressures, is at the root of a substantial redshift with respect to the typical free OH stretching frequency, which eludes its straightforward detection.

Introduction

Titania surfaces have many important applications in biochemistry, catalysis or as functional materials. Many of them can be tuned by the preparation conditions and the chemical environment (in particular, oxidizing or reducing conditions).[1] Nowadays, TiO_2 surfaces are rather well controlled and characterized, and numerical simulations are employed to study their reactivity, from water splitting[2–5] to more complex reactions with biomolecules.[6]

Among the open problems, a prominent issue is represented by the adsorption of carboxylic acids (R-COOH), which are employed to anchor dye sensitizers to titania. As carboxylic acids are among the simplest organic acids, they also represent prototypes for probing the reactivity of TiO_2 surfaces. The knowledge of the adsorption process at the atomic scale is thus a prerequisite for designing and modelling more complex reactions in photocatalysis. While there is a consensus that the most stable adsorption sites are the under-coordinated surface Ti (Ti_n, with $n \leq 5$), the interaction between the surface oxygen atoms O_s and the carboxylic group is far from being fully understood and unambiguously characterized. More specifically, it has been observed that formic acid adsorbs in a dissociated formate specie on most TiO_2 surfaces, including rutile (110)[7] and anatase (001)[8] ones. In spite of the vast amount of work (both experimental and theoretical) performed, it is still under debate whether the formic acid adsorption on the anatase (101) surface is molecular or dissociative. Formic acid can bind to the most stable anatase (101) surface either through an oxygen end in the monodentate (M) configuration, or through two oxygen ends in the bridging bidentate (BB) configuration. This last one is dissociated and we refer to it as BB(H), while the monodentate one instead can be either in molecular form, i.e. without proton dissociation (MH), or without the proton, after its dissociation from the ad-molecule, M(H) (Figure 1a). Experiments and first-principle calculations suggest the presence of both monodentate and bridging bidentate conformers.[9–15]

Recent ab initio classical molecular dynamics[14] focused on the molecular monodentate conformer where the adsorbed formic acid forms a short hydrogen bond with a surface oxygen O_s, along which the proton can be shared between the carboxyl group and the anatase surface. The authors found that the barrier between the two localized configurations (that is, H^+ either on the ad-molecule or on the surface oxygen) is smaller than the proton zero-point energy (ZPE), making the proton shuttle freely between the carboxyl group and the surface oxygen, so to preserve the Brønsted-acid functionality of the molecule.

The previous scenario leaves two pending questions: (i) the adsorption mode of the formic acid and (ii) the localization of the proton following the adsorption. Answering to them is the main goal of this work and this is potentially relevant for all carboxylic compounds in photocatalysis, where the interaction between the surface oxygen ions and the carboxylic group can determine the issue of the catalytic process.

The main limitations to know where the acid proton is[14] stem from the proton high mobility, which is due to its charge, its small size and appreciable de Broglie thermal wavelength (about 1 Å at room temperature). Calculations

[*] E. Fallacara, F. Finocchi, S. Chenot, S. Stankic
Institut des NanoSciences de Paris (INSP), Sorbonne Université, CNRS UMR 7588, 4 Place Jussieu, 75252 Paris, France
E-mail: slavica.stankic@insp.jussieu.fr
M. Cazzaniga, M. Ceotto
Dipartimento di Chimica, Università degli Studi di Milano, Via C. Golgi 19, 20133 Milano, Italy
E-mail: michele.ceotto@unimi.it

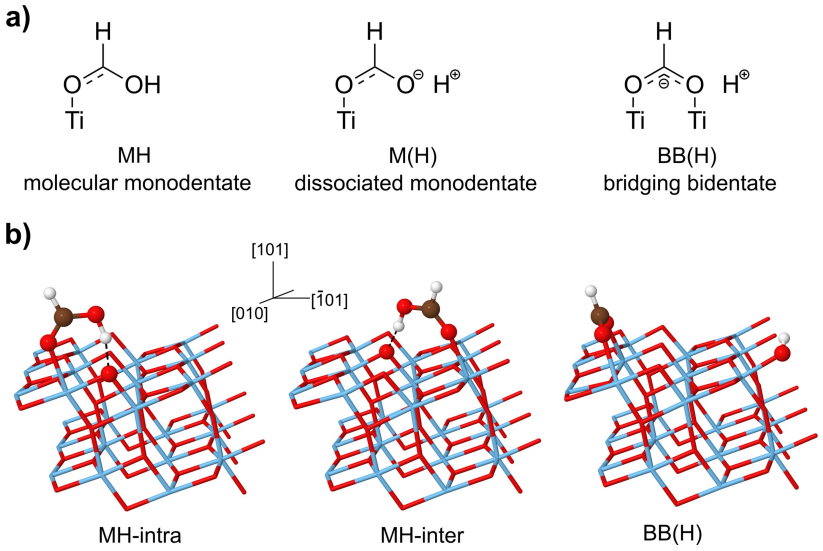

Figure 1. a) Sketches of the formic acid conformers on the anatase (101) surface. b) Representation of the three minima on the anatase (101) surface and the crystal axes. The surface adsorption sites are the Ti atoms. The two monodentate configurations (MH-intra, MH-inter) differ by their orientation with respect to the surface.

relying only on classical optimizations (accounting neither for thermal nor quantum effects), where the stability on an absolute scale is the energy at the bottom of the potential well, have not come to a consensus on the stable adsorption configurations of formic acid on anatase (101) surface. Actually, the interpretation of the experimental results on the basis of the available calculations is still equivocal, especially concerning the fate of the acid proton.

In order to overcome this deadlock, we devised a joint experimental and theoretical approach. On one side, we measured low-temperature infrared spectra in ultrahigh vacuum (UHV) conditions on well controlled titania nanopowders; their very large surface-to-bulk ratio makes them suitable for highly surface-sensitive experiments. Infrared (IR) spectroscopy is particularly useful to monitor the behavior of hydrogen, as the vibrations of the hydroxyl signals are affected by hydrogen bonds. On the other side, we carried out density functional theory (DFT) based simulations where the quantum nature of the proton is fully taken into account, both for the equilibrium properties, via path-integral molecular dynamics (PIMD),[16] and for the vibrational properties, via divide-and-conquer semi-classical initial value representation (DC-SCIVR),[17–19] which are able to describe anharmonic coupling and nuclear quantum effects on the dynamics.

We will show that this strategy can solve the issue of the fate of the proton following the HCOOH adsorption on the anatase (101) surface. Here, particularly puzzling is the fact that the ν(OH) stretching mode signal of HCOOH on anatase (101) has not been detected so far. For this reason, we carried out complementary experiments for the adsorption of deuterated formic acid HCOOD. The comparison between the IR signals of HCOOH and HCOOD from very low (13 K) to room temperatures allows to identify the features that are specific to the acid proton (or deuteron) and to point out the quantum effects, which are sensitive to the particle mass. In this way, we will be able to identify the proton (deuteron) IR signals and infer their location on the surface, which can be either on the original molecular site or on a surface oxygen.

Finally, we characterize the hydrogen bond occurring between the formic acid and the anatase surface, which, we anticipate, is quite peculiar and has eluded a precise description up to now. Specifically, two effects on the stretching mode frequency ν(OH) are usually related to the formation of H bonds: (i) a detectable red-shift, which stems from the dilatation of the covalent OH bond; (ii) a significant enhancement of its integrated IR intensity, which originates from the large variation of the electric dipole moment along the asymmetric stretch direction.[20] Those two characteristics are consistently accounted for by semi-classical simulations, which therefore are very effective to complement and interpret the measured IR spectra.

Our starting point was the classical optimization at $T=$ 0 K. The optimized minima are shown in Figure 1b, on the top of the (101) sawtooth-like anatase most stable surface. Among the monodentates, the acid proton can form a hydrogen bond with the twofold-coordinated surface O_s atom either along the same chain of the Ti_{5c} adsorption site (MH-intra) or across a neighboring chain (MH-inter). The comparison of the binding energies as obtained within the Perdew–Burke–Ernzerhof (PBE) functional[21] shows that two monodentate forms are almost degenerate (MH-intra is 0.01 eV more stable than MH-inter), and 0.15 eV more stable than the BB(H) form. Static calculations therefore suggest that the preferred adsorption modes are the MH-inter and MH-intra. The same vibrational frequency picture described below for the adsorbed molecule can be obtained by employing van der Waals potential corrections in the DFT functional, as described in Section 2.4 of the Supporting Information.

In analogy with previous studies on proton sharing in various systems,[22–24] we analyze the acid proton potential energy surface (PES) as a function of the coordinate $\delta = r_2 - r_1$, by relaxing all the degrees of freedom at constrained δ. The parameter r_1 is the OH bond length in the formic acid and r_2 is the distance of the proton from the nearest surface oxygen O_s (that is, the H bond length) (Figure 2a). The PES for the MH-intra configuration (Figure 2b) shows an asymmetric single well with a minimum corresponding to the proton bound to the molecule ($\delta \simeq 0.5$). The single-well picture stands even if the detailed PES shape is sensitive to the positions of the other atoms, especially of the second H neighbors. We anticipate that the zero-point energy of the OH stretching mode amounts to $\simeq 0.18$ eV. The proton thus does not remain at the bottom of the potential well and classical theory is not adequate to describe its localization and dynamics.

The difference of the electron density between the proton at the bottom of the well ($\delta \simeq 0.5$) or centred ($\delta = 0$) is clearly visible in Figure 2c. As the proton can be significantly delocalized,[22] determining its mean distribution by taking into account its quantum nature is therefore essential to obtain a consistent interpretation of the role of the surface in photocatalysis.

In order to characterize the formic acid adsorption, we analyze the infrared spectra of the adsorbed formic acid (Figure 3), separately for two spectral ranges: (i) $1000\ \text{cm}^{-1} \leq \nu \leq 1800\ \text{cm}^{-1}$ and (ii) the *high-frequency region* $\nu \geq 2000\ \text{cm}^{-1}$. We refer to the former frequency domain as the *fingerprint region*: this is the characteristic range for the vibrational modes involving the C and O atoms of the formic acid, which differ between the BB(H) adsorption configuration (that has a mirror symmetry) and the monodentate ones. The high-frequency range is characteristic of OH and OD modes and yields direct information about the possible proton (deuteron) dissociation.

In the *fingerprint region*, the HCOOH and HCOOD spectra are very similar to each other, which shows that the deuteration does not influence the adsorption mode. At 13 K, the spectra show a prominent peak either at 1250 cm^{-1} (HCOOH) or 1257 cm^{-1} (HCOOD). Those frequencies can be interpreted as due to a single C–O bond, as for the monodentate configurations. At room temperature, both HCOOH and HCOOD spectra also show the typical frequencies of the symmetric (1320 cm^{-1}) and anti-symmetric (1555 cm^{-1}) O–C–O modes, the latter peak being more intense than the former, consistently with its much larger dipole strength. At the same time, one can note the persistence of a shoulder at $\simeq 1250\ \text{cm}^{-1}$. Therefore, the

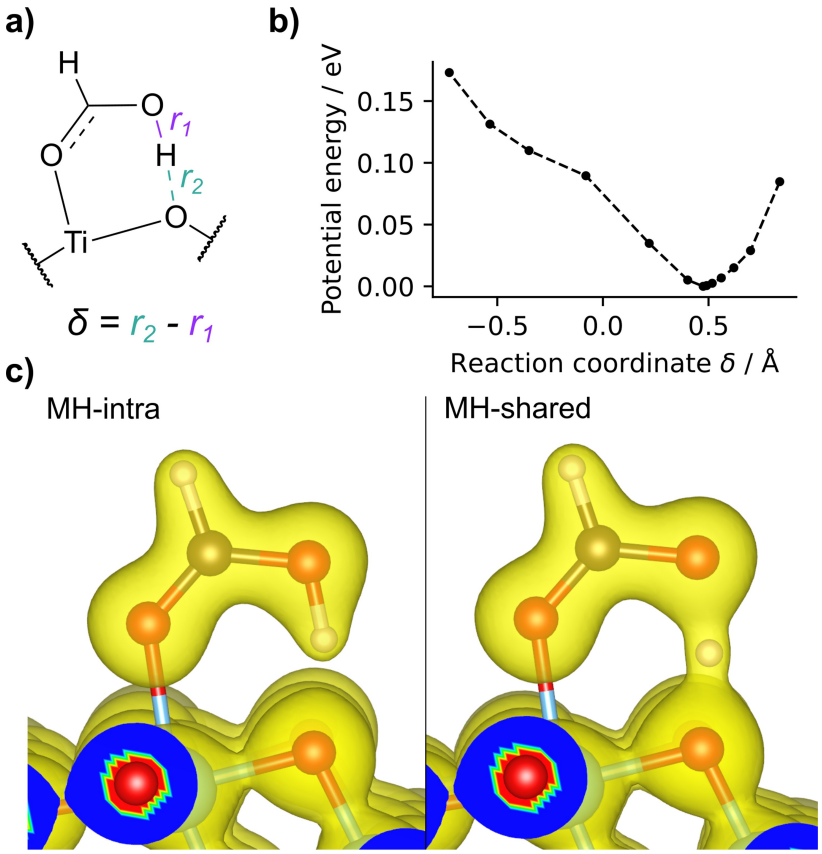

Figure 2. a) Sketch of the MH adsorption configuration with the definition of the r_2 and r_1 coordinates. b) The classic $T = 0$ K potential energy surface as obtained through constrained minimization at fixed $\delta = r_2 - r_1$. All degrees of freedom other than δ are relaxed. c) The electron density as obtained for the stable MH-intra ($\delta \simeq 0.5$) and the proton-shared ($\delta = 0$) configurations. The transparent orange density surface is drawn at 0.1 electrons/Å^3.

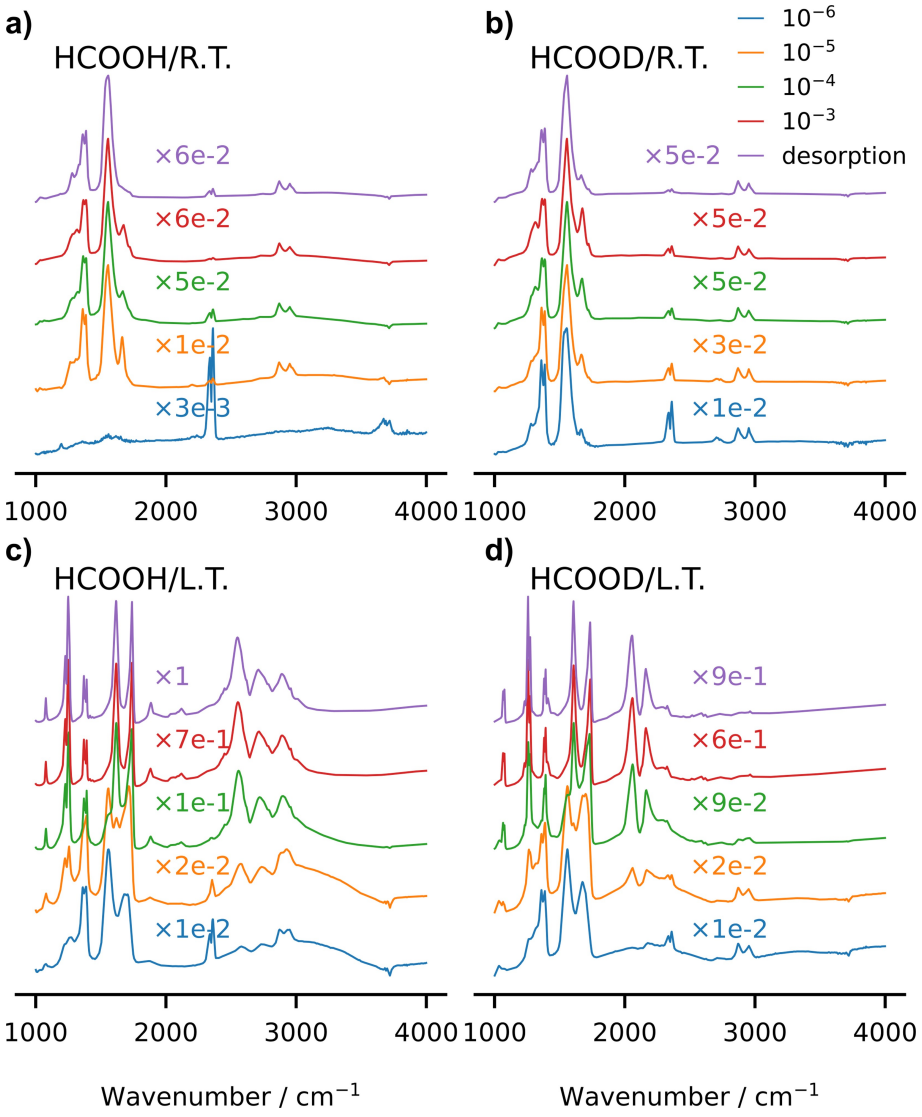

Figure 3. Measured UHV Fourier Transform Infra-Red (FTIR) spectra for protonated HCOOH and deuterated HCOOD formic acid on anatase nanopowders. The spectra are recorder either at room temperature (R.T.) or at low temperature (L.T.), $T = 13$ K, and at various formic acid partial pressures, from 10^{-6} to 10^{-3} mbar up to the desorption limit.

spectra suggest that the prominent adsorption configuration is the monodentate one at low temperature, while both mono- and bi-dentate configurations coexist at room temperature.

In the *high-frequency region*, firstly we focus on the spectra that have been recorded at low partial pressure ($P = 10^{-5}$ mbar) and low temperature ($T = 13$ K), for both HCOOH and HCOOD, drawn as orange lines in the lower panels of Figure 3. The twofold signal at 2890 and 2955 cm^{-1} (HCOOD) or 2890 and 2940 cm^{-1} (HCOOH), thus very similar in the two species, is due to the C–H stretching mode. The higher peak is probably related to a combination band, as already pointed out.[25] Note that there are no signals above 3000 cm^{-1}, in the typical range of the hydroxyl stretching mode, apart from a small structure (negative with respect to the baseline) whose main peak is around 3700 cm^{-1}. We ascribe it to the presence of residual free (not H-bonded) hydroxyl groups that were present on the as-prepared nanopowders and left the surfaces upon formic acid adsorption; afterwards, there is no trace of the expected OH stretching vibrations. This puzzling absence poses the problem of the fate of the formic acid proton, which cannot be elucidated just by looking to the measured IR spectra. In order to solve the issue and identify the acid proton signal, we resort to theory, first employing the harmonic analysis and then using DC-SCIVR.

For the most stable configurations as obtained from geometry optimization (Figure 1, lower panel), the computed harmonic stretching modes for the two MH configurations (MH-intra and MH-inter) are represented by vertical dashed lines in Figures 4b and 4c. The OH harmonic stretching lies at 2532 (MH-intra) and 2592 cm^{-1} (MH-inter) and its OD counterparts at 1872 (MH-intra) and 1919 cm^{-1} (MH-inter). In both cases, a striking effect is the amount of

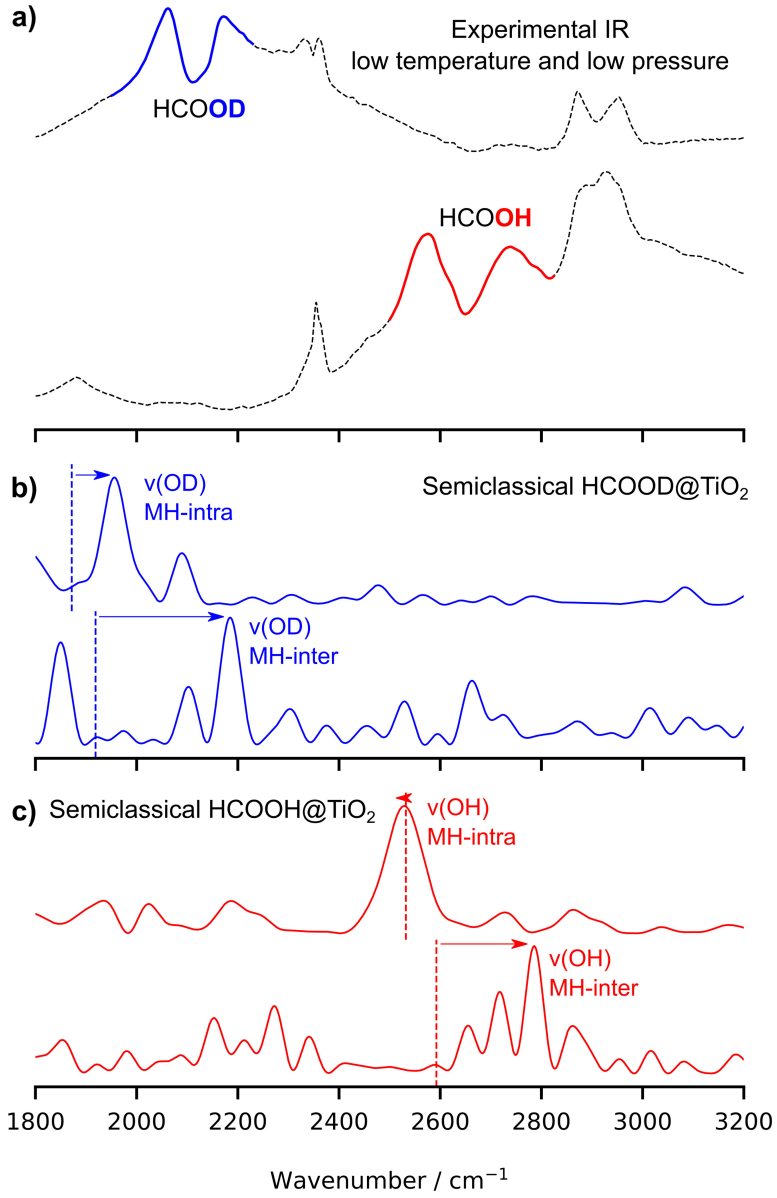

Figure 4. The assignment of the acid proton signal. a) The experimental UHV FTIR at 13 K for HCOOH and HCOOD in the 1800–3200 cm^{-1} spectral range at partial pressure $P = 10^{-5}$ mbar. b) The computed signal related to the OD adsorbed formic acid group in the MH-intra and MH-inter configurations. c) Same as above for the OH adsorbed formic acid group. Vertical dashed line are the harmonic estimates.

red-shift that formic acid undergoes after adsorption with respect to the original gas-phase $\nu_s(OH)$ frequency, which is around 3570 cm^{-1}. Indeed, the formation of a hydrogen bond weakens the covalent bond and induces a giant red-shift ($\simeq -1000$ cm^{-1}), which is comparable to what obtained at the ice VII–X transition at 60 GPa pressure,[23] in extreme conditions that contrast from those of the present measurements. Such a red-shift has been suggested by Tabacchi and co-workers,[14] on the basis of the Fourier analysis of classical molecular dynamics trajectories, but without any specific assignment.

The experimental IR spectra show a complex twofold structure, with small maxima at 2576 and 2737 cm^{-1} in HCOOH, and two asymmetric maxima at 2060 and 2172 cm^{-1} in HCOOD, the latter one with a broad tail extending up to higher frequencies. These frequencies are thus sensitive to isotope substitution and potential candidates for the OH/OD stretching modes. In order to find the OH/OD fundamental signal, we employ suitable combinations of coherent states in our semiclassical method, as detailed in the Supporting Information. A direct comparison of the DC-SCIVR OH/OD signals with the experimental spectrum (Figure 4) allows to highlight the part in the experimental spectrum which can be attributed to the OD (blue) and OH (red) fundamental stretching modes. They come out as the most prominent peaks among other structures that are due to anharmonic coupling: $\nu(OH) \sim 2550$ cm^{-1} for the MH-intra and

ν(OH) ~ 2740 cm^{-1} for the MH-inter. Analogously for the deuterated form, we assign ν(OD) ~ 2055 cm^{-1} for the MD-intra and ν(OD) ~ 2160 cm^{-1} for the MD-inter. From the comparison, we conclude that at low temperature and small partial pressure (thus in the regime of almost isolated adsmolecules), the formic acid adsorbs preferentially in the two monodentate configurations. The acid proton (deuteron) binds to the molecule, although a strong hydrogen bond forms with the surface O ion, which considerably weakens the OH (OD) covalent bonds and is responsible for the anharmonic and quantum effects on the hydrogen dynamics. Actually, our semiclassical method simulates the quantum power spectrum and it provides the collection of all the vibrational eigenvalues on an absolute scale. For the sake of comparison with the experimental IR spectra, in Figures 4b and 4c we shifted the lowest eigenvalue (i.e. the ZPE) to zero. In the DC-SCIVR procedure, the vibrational space is divided in vibrational subspaces, so that the modes belonging to the same subspace of the OH/OD stretching mode show a significant coupling with the former one. Accordingly, in Figures 4b and 4c we collect the vibrational eigenvalues (fundamentals, combination bands and overtones) that are mostly coupled to the OH/OD stretching motion. Additional power spectra for the gas-phase, the MX-intra, MX-inter, and the BB(X) (X=H, D) forms are reported in the Supporting Information (Figure S7). There, the available experimental frequencies are reported as red rectangols and the accuracy of our computational set-up is quite good for the main formic acid modes.

In all but the MH-intra case, the semiclassical frequencies are larger than their harmonic counterparts: anharmonic and quantum contributions yield a significant blue-shift to the harmonic frequencies. This counterintuitive effect will be analyzed later on. We also stress that the semiclassical spectra show that the OH and OD stretching modes couple with other modes, on the surface and on the molecule. This is consistent with the proton PES sensitivity to the motion of the neighboring atoms, in particular the O ions the proton binds to.

At room temperature (see Figure 3), we observe that the C–H stretching related signal is clearly visible as a twofold structure in both HCOOH and HCOOD, with peaks at similar frequencies as at low temperature. In contrast, the signals corresponding to the O–H (O–D) stretching modes are much attenuated with respect to 13 K and hardly visible at 10^{-5} mbar pressure. However, when looking to spectra that have been measured at room temperature and higher pressures (between 10^{-4} and 10^{-3} mbar), the upper maxima appear at similar frequencies as at low temperature: 2169 cm^{-1} (OD stretching) and 2734 cm^{-1} (OH stretching). Interestingly, the positions of the lower maxima are slightly sensitive to the temperature, as they show up at 2111 cm^{-1} in HCOOD and $\simeq$ 2600 cm^{-1} in HCOOH. In synthesis, we can therefore assign, by means of the DC-SCIVR computed spectra, the measured twofold IR signals around $\simeq$ 2650 cm^{-1} for HCOOH and $\simeq$ 2100 cm^{-1} for HCOOD as mainly due to the OH (OD) stretching in the MH-intra and MH-inter configurations.

Once the experimental spectra have been interpreted and the O–H (O–D) has been assigned, a question still remains unanswered, about the strong and unusual hydrogen bond between the adsorbed formic acid and the anatase (101) surface and the blue-shift of the frequencies with respect to the harmonic estimates.

In Figure 5b, we compare the classical and quantum distributions of the quantum proton and deuteron as a function of the proton-sharing coordinate $\delta = r_2 - r_1$ at $T =$ 100 K. Our PIMD simulations show that the proton- and deuteron-sharing between the formic acid and the surface is enhanced by quantum effects, especially for the lighter proton, which has a broader and more asymmetric distribution than the deuteron. The PIMD simulations disclose the zero point energy contribution as the main quantum mechanical effect contributing to the proton and deuteron quantum delocalization.

Such a proton-sharing is representative of what is needed for activating the photocatalytic oxide surface decomposition of carboxylic acids. In order to evaluate it more quantitatively, we compare proton sharing in FA/anatase to the gas-phase Zundel cation and the formic acid dimer (FAD), through the corresponding quantum distributions (Figure 5c). The larger delocalization occurs in the Zundel cation, where the proton is equally shared between the two water molecules. In contrast, in the gas-phase formic acid dimer, the proton is clearly more localized on one side of the dimer. The adsorbed formic acid on the anatase (101) surface lies in between the previous cases: although it is more on the molecule side ($\delta > 0$) the distribution indicates a non negligible probability to lie closer to the surface O than to the O in the molecule ($\delta < 0$). The proton is as delocalized as in the Zundel ion, but its distribution is skewed, consistently with the absence of mirror symmetry.

These considerations are further supported by a coarse vibrational frequency consideration. In the FAD, the main OH stretch peak is located at ~3200 cm^{-1}, while the Zundel cation proton shuttling mode vibrates at ~1000 cm^{-1}; for the adsorbed formic acid, the proton stretching mode is at ~ 2600 cm^{-1} (Figure 4).

This clearly shows the importance of the surface and quantifies its role in a chemical scale by comparison with other compounds. One could also put forward a one-dimensional picture by comparing the PES along the MH-intra OH stretch direction and the harmonic potential shape of other compounds characterized by different molecular interactions, as we did in the Supporting Information (Section 3.3). However, we find that this picture is not clearly explaining the anharmonic blue shift because it is limited to a one-dimensional potential profiling. We have also investigated if the phonon modes which are more coupled to the molecules are somehow more localized than then others. Section 3.4 of the Supporting Information shows that this is true only in part.

Eventually, the fate of the proton is now clear. The proton is confined to vibrate between the molecule and surface O atoms. The distance between these atoms is very short (~2.5–2.6 Å) due to the strong hydrogen bond between the molecule and the titania surface, which causes a large

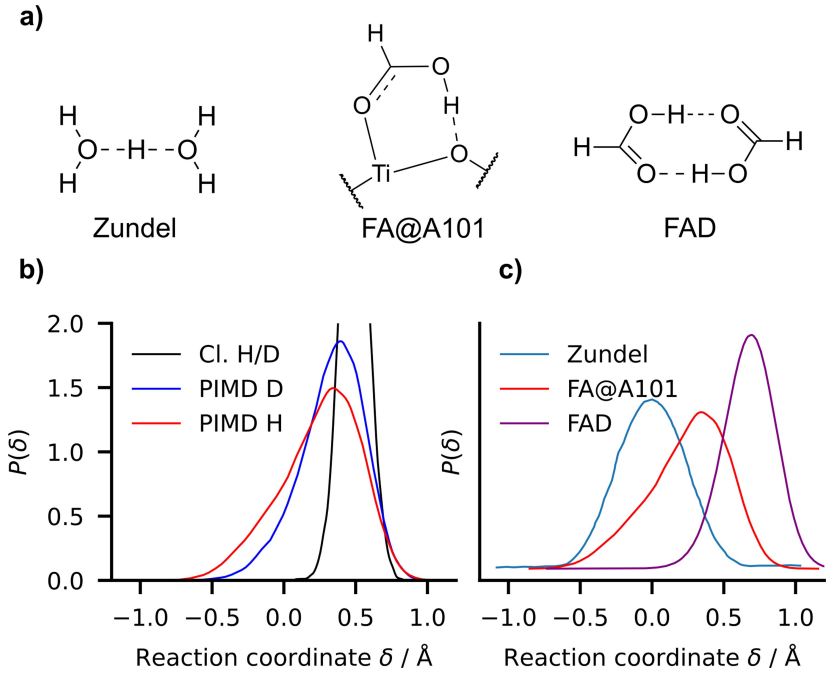

Figure 5. The zero point energy quantum delocalization. a) Proton-sharing structures chemical formulas of the Zundel cation, the formic acid on the anatase (101) surface (FA@A101) in the MH-intra configuration and formic acid dimer (FAD) in the gas phase. b) Proton probability distributions as function of $\delta = r_2 - r_1$ at $T = 100$ K: classical (Cl.) vs quantum (PIMD) proton-sharing distribution functions in FA@A101. HCOOH is label as "H" and HCOOD as "D". c) PIMD probability distribution at $T = 100$ K of proton sharing coordinate δ in Zundel cation from Shran et al.[26] (Figure 4, curve at 2.4 Å), formic acid adsorbed on anatase FA@A101 and formic acid dimer FAD using PES from Qu et al.[27] The O–O average equilibrium distance is 2.40 Å, 2.47 Å and 2.68 Å in the Zundel cation, FA@A101 and FAD, respectively. The condition $\delta > 0$ implies that the proton is closer to the molecule than to the surface.

frequency red-shift ($\sim -1000\ \mathrm{cm}^{-1}$) with respect to the free O–H typical signal. In addition, since the proton is driven by a very strong H-bond, comparable to those in ice at high pressure (> 20 GPa), it experiences quite an unusual potential characterized by a low frequency and it is less confined respect to an ordinary OH-stretch. The small blue shift observed may be compatible with this quantum picture where the proton shuttle at a significant zero point energy value and with a wider amplitude, like a particle-in-a-box, the vibrational energy spacing is increasing with the quantum number.

To summarize, we studied the formic acid adsorption on the (101) anatase surface, which is at the same time a prototype for probing the proton affinity of surface O sites and a challenging system to obtain a consistent understanding of the reaction with carboxyls. We recorded UHV infrared spectra from room temperature down to temperatures as low as 13 K, and for various formic acid partial pressures, both for HCOOH and HCOOD. For reaching a consistent atomic-scale picture of these processes, we go beyond static DFT calculations, including quantum effects on the nuclear distributions via Feynman path integrals and on the vibrational motion via semiclassical molecular dynamics, coming to the following main conclusions. (i) The formic acid adsorbs in the molecular monodentate configurations at low temperatures, while the bridging bidentate configuration is present at room temperature. (ii) We locate the acid proton on the ad-molecules and assign the related OH stretching signal at $\simeq 2700\ \mathrm{cm}^{-1}$, in agreement with previous ab initio results.[14] (iii) We exclude the presence of dissociative monodentate adsorption, with the proton on a surface O site, which would yield a much higher OH stretching frequency than experimentally detected. (iv) The formic acid forms an exceptionally strong H bond with the surface oxygen and its vibrational motion is characterized by a huge $\simeq 1000\ \mathrm{cm}^{-1}$ red shift respect to the free OH-stretch. (v) Finally, the strength of the H bond is at the root of the unusual low frequency of the OH stretching mode and the quantum proton dynamics is experiencing that reminds that of hydrogen bonds at high pressure.

In conclusions, the anatase (101) surface behaves as an *incomplete* base in the Brønsted's sense, as the acid proton, although strongly bound to the surface, is not transferred to it. This explains why the acid proton is not detected by the scanning tunneling microscopy, since the carboxylate group could conceal it from the tip.[28]

Acknowledgements

This work was granted access to the high-performance computing resources of CINES under the allocation A019096719 and of TGCC under the allocation A0210906719, both made by GENCI. M. Cazzaniga and M. Ceotto acknowledge financial support from the European Research Council (Grant Agreement No. 647107 SEMI-

COMPLEX ERC-2014-CoG) under the European Union's Horizon 2020 research and innovation programme, and from the Italian Ministery of Education, University, and Research (MIUR) (FARE programme R16KN7XBRB – project QURE). E.F. acknowledges her PhD fellowship by *École Doctorale 397 - Physics and Chemistry of Materials.* The authors warmly thank Claudine Noguera for the critical reading of the manuscript, as well as Philippe Depondt and Simon Huppert for useful discussions and continuous support. Open Access publishing facilitated by Università degli Studi di Milano, as part of the Wiley - CRUI-CARE agreement.

Conflict of Interest

The authors declare no conflict of interest.

Data Availability Statement

The data that support the findings of this study are available from the corresponding author upon reasonable request.

Keywords: Carboxylic Acid Adsorption · Anatase Nanoparticles · Infrared Spectroscopy · Semiclassical Dynamics · Quantum Effects

[1] U. Diebold, *Surf. Sci. Rep.* **2003**, *48*, 53–229.
[2] M. Ni, M. K. Leung, D. Y. Leung, K. Sumathy, *Renewable Sustainable Energy Rev.* **2007**, *11*, 401–425.
[3] M. Cazzaniga, M. Micciarelli, F. Gabas, F. Finocchi, M. Ceotto, *J. Phys. Chem. C* **2022**, *126*, 12060–12073.
[4] M. F. C. Andrade, H.-Y. Ko, L. Zhang, R. Car, A. Selloni, *Chem. Sci.* **2020**, *11*, 2335–2341.
[5] F. Fasulo, G. Piccini, A. B. Muñoz-García, M. Pavone, M. Parrinello, *J. Phys. Chem. C* **2022**, *126*, 15752–15758.
[6] T. Tarjànyi, F. Bogàr, J. Minàrovits, M. Gajdàcs, Z. Tóth, *PLoS One* **2023**, *18*, e0289467.
[7] A. Mattsson, S. Hu, K. Hermansson, L. O" sterlund, *J. Vac. Sci. Tech. A* **2014**, *32*.
[8] X.-Q. Gong, A. Selloni, A. Vittadini, *J. Phys. Chem. B* **2006**, *110*, 2804–2811.
[9] M. Nilsing, S. Lunell, P. Persson, L. Ojamäe, *Surf. Sci.* **2005**, *582*, 49–60.
[10] A. Vittadini, A. Selloni, F. Rotzinger, M. Grätzel, *J. Phys. Chem. B* **2000**, *104*, 1300–1306.
[11] R. Luschtinetz, S. Gemming, G. Seifert, *Eur. Phys. J. Plus* **2011**, *126*, 98.
[12] M. Xu, H. Noei, M. Buchholz, M. Muhler, C. Wo"ll, Y. Wang, *Catal. Today* **2012**, *182*, 12–15.
[13] L. Kou, T. Frauenheim, A. Rosa, E. Lima, *J. Phys. Chem. C* **2017**, *121*, 17417–17420.
[14] G. Tabacchi, M. Fabbiani, L. Mino, G. Martra, E. Fois, *Angew. Chem. Int. Ed.* **2019**, *58*, 12431–12434.
[15] Y. Wang, B. Wen, A. Dahal, G. A. Kimmel, R. Rousseau, A. Selloni, N. G. Petrik, Z. Dohnálek, *J. Phys. Chem. C* **2020**, *124*, 20228–20239.
[16] D. Marx, M. Parrinello, *J. Chem. Phys.* **1996**, *104*, 4077–4082.
[17] C. Aieta, M. Micciarelli, G. Bertaina, M. Ceotto, *Nat. Commun.* **2020**, *11*, 1–9.
[18] F. Gabas, G. Di Liberto, R. Conte, M. Ceotto, *Chem. Sci.* **2018**, *9*, 7894–7901.
[19] A. Rognoni, R. Conte, M. Ceotto, *Chem. Sci.* **2021**, *12*, 2060–2064.
[20] A. C. Legon, D. J. Millen, *Faraday Discuss. Chem. Soc.* **1982**, *73*, 71–87.
[21] J. P. Perdew, J. A. Chevary, S. H. Vosko, K. A. Jackson, M. R. Pederson, D. J. Singh, C. Fiolhais, *Phys. Rev. B* **1992**, *46*, 6671–6687.
[22] M. Benoit, D. Marx, *ChemPhysChem* **2005**, *6*, 1738–41.
[23] Y. Bronstein, P. Depondt, F. Finocchi, A. M. Saitta, *Phys. Rev. B* **2014**, *89*, 214101.
[24] Y. Bronstein, P. Depondt, F. Finocchi, *Eur. J. Mineral.* **2017**, *29*, 385–395.
[25] N. G. Petrik, Y. Wang, B. Wen, Y. Wu, R. Ma, A. Dahal, F. Gao, R. Rousseau, Y. Wang, G. A. Kimmel, et al., *J. Phys. Chem. C* **2021**, *125*, 7686–7700.
[26] C. Schran, F. Brieuc, D. Marx, *J. Chem. Theory Comput.* **2018**, *14*, 5068–5078.
[27] C. Qu, J. M. Bowman, *J. Chem. Phys.* **2018**, *148*, 241713.
[28] D. C. Grinter, M. Nicotra, G. Thornton, *J. Phys. Chem. C* **2012**, *116*, 11643–11651.

Manuscript received: May 20, 2024
Accepted manuscript online: July 30, 2024
Version of record online: ■■, ■■

Research Article

Surface Chemistry

E. Fallacara, F. Finocchi, M. Cazzaniga,
S. Chenot, S. Stankic,*
M. Ceotto* _____ **e202409523**

The Fate of the Formic Acid Proton on the Anatase TiO_2(101) Surface

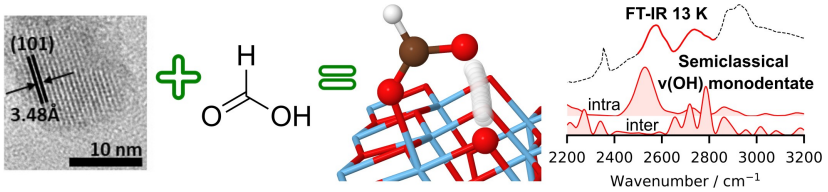

High vacuum FTIR experiments at temperatures as low as 13 K, together with divide-and-conquer semiclassical and path integral molecular dynamics simulations, indicate that a short and strong hydrogen bond is formed during the adsorption of HCOOH on the anatase (101) TiO_2 surface. Such unusual H-bond has previously escaped direct spectral detection because of a huge red shift of its vibrational frequency.

@CeottoGroup

Share your work on X! Angewandte Chemie promotes selected articles on X (formerly known as Twitter). Each article post contains the title, name of the corresponding author, a link to the article, selected handles and hashtags, and the ToC picture. If you, your team, or your institution have an X account, please include its handle @username below. We recommend sharing and interacting with these posts through your personal and/or institutional accounts to help increase awareness of your work! Please follow us @angew_chem.

Please check that the ORCID identifiers listed below are correct. We encourage all authors to provide an ORCID identifier for each coauthor. ORCID is a registry that provides researchers with a unique digital identifier. Some funding agencies recommend or even require the inclusion of ORCID IDs in all published articles, and authors should consult their funding agency guidelines for details. Registration is easy and free; for further information, see http://orcid.org/.

Erika Fallacara http://orcid.org/0000-0002-3487-5572
Fabio Finocchi http://orcid.org/0000-0002-7048-5029
Marco Cazzaniga http://orcid.org/0000-0002-8473-0574
Stéphane Chenot
Slavica Stankic http://orcid.org/0000-0002-8711-9746
Michele Ceotto http://orcid.org/0000-0002-8270-3409